International Journal of Science and Research (IJSR)
ISSN (Online): 2319-7094
Index Copernicus Value (2015): 78.96 | Impact Factor (2015): 6.391

Enhanced Yellow Luminescence from $LaAlO_3:Sm^{3+}$ [Li^+, Na^+, K^+, Ag^+] Nano-Phosphors Prepared by Combustion Synthesis

Subhash Chand[1], Ishwar Singh[2]

[1]Department of Chemistry, Maharshi Dayanand University, Rohtak-124001, Haryana, India

[2]PDM University, Sector 3A, Sarai Aurangabad, Bahadurgarh-124507, Haryana, India

Abstract: ***$LaAlO_3:Sm^{3+}$, [Li^+, Na^+, K^+, Ag^+] nano-phosphors with varying dopant concentrations of Sm^{3+} from 1 to 20 mol% & codopants concentration of [Li^+, Na^+, K^+, Ag^+] is 0.5 to 1 mol% were prepared by combustion synthesis method and the samples were further heated to 600,700, and 1000 ^{0}C to improve the crystallinity of the materials. The structure and morphology of materials have been examined by X-ray diffraction and scanning electron microscopy. XRD results reveal that the sample begins to crystallize at 600°C , and pure $LaAlO_3$ phase can be obtained at 700°C. SEM images indicate that the Sm^{3+} -doped LaAlO3 phosphors are composed of aggregated spherical particles with sizes ranging from 40 to 80nm . Under the excitation of UV light (245nm) and low-voltage electron beams (1–3kV) , the Sm^{3+} -doped $LaAlO_3$ phosphors show the characteristic emissions of phosphor consist of five emission peaks, which are attributed to the transitions from $^4G_{5/2}$ state to ^6H_J (J=5/2, 7/2, 9/2, 11/2 ,13/2) states of Sm^{3+} ions with Yellow, Yellow-orange and Orange-red color. Among these, emission peak located at 563, 598, 611, 653, 707 nm are attributed to the transitions of $^4G_{5/2}\rightarrow{}^6H_{5/2}$, $^4G_{5/2}\rightarrow{}^6H_{7/2}$, $^4G_{5/2}\rightarrow{}^6H_{9/2}$, $^4G_{5/2}\rightarrow{}^6H_{11/2}$ & $^4G_{5/2}\rightarrow{}^6H_{13/2}$ respectively. Among these emission peaks, the transition emission $^4G_{5/2}\rightarrow{}^6H_J$ (J=5/2, 7/2, 9/2) for peak at 563, 598, 611nm is strongest for Yellow, Yellow-orange and strong Orange-red emission is due to the magnetic dipole transition of Sm^{3+} ion having a magnetic dipole (MD) allowed one and also an electric dipole (ED) dominated one but the other weak transition $^4G_{5/2}\rightarrow{}^6H_{11/2}$ & $^4G_{5/2}\rightarrow{}^6H_{13/2}$ (653 nm, 707nm red) is purely an ED one. Highest photoluminescence intensity is observed with 3 mol% doping of (Sm^{3+}+ Na^+=3mol% for promising Yellow) (Sm^{3+}+ K^+=3mol%, for Yellow-orangish, Orangish-red) , made $LaAlO_3:Sm^{3+}$, [Li^+, Na^+, K^+, Ag^+] a strong competitor for promising Yellow, Yellow-orange & also for Orange-red colored display applications.***

Keywords: Combustion synthesis, Nano-phosphors, $LaAlO_3:Sm^{3+}$, [Li^+, Na^+, K^+, Ag^+], Host lattices, Codopants, Magnetic dipole, Electric dipole

1. Introduction

More recently, however, the development of flat panel displays, such as field emission displays (FEDs), plasma display panels (PDPs) and thin film electro-luminescent devices (TFEL), or white light emitting diode (LED), have emerged as the principal motivation for research into rare-earth luminescence, and the present article therefore concentrates on the variety of different ways in which rare-earth luminescence has been exploited in this field[1–4] . The rare-earth ions are characterized by a partially filled 4f shell that is well shielded by $5s^2$ and $5p^6$ orbitals. The emission transitions, therefore, yield sharp lines in the optical spectra. The use of rare-earth element based phosphor, based on "line-type" f–f transitions,[5-7] can narrow to the visible, resulting in both high efficiency and a high lumen equivalent [8]. It is, therefore, urgent to find a stable, inorganic rare-earth-based phosphor with high luminescent efficiency. The phases composed by the elements with the smaller difference of electronegativity (X), corresponds to a narrower band gap of compounds, leading to higher conductivity. The difference between the electronegativities of Si and O (X= 1.54) exceeds that between Ge and O (X= 1.43)[9]. During the past decades, rare earth ions doped in various host materials have been widely studied due to their characteristic luminescence properties. Among the rare earth ions,Sm^{3+} ,Eu^{3+} , Tb^{3+} , and Dy^{3+} are important activator ions for producing visible light [10–17]. Sm^{3+} activated luminescent materials have received much attention at present [18-19]. They show bright emissions in orange and red regions attributed to the transitions from the excited state $^4G_{5/2}$ to the ground state $^6H_{5/2}$ and the other state ^6H_J (J = 7/2, 9/2 , and 11/2), which can be used in high density optical storage, temperature sensors, under sea communication, various fluorescent devices, color display, and visible solid-state lasers [20–21]. Luminescence of is especially useful to probe the local structure of luminescent centers in a host lattice because of its simple energy level structure, great sensitivity to ligand field, and similar lanthanide chemical properties to the other rare earth ions [22-23]. Growing interest recently has been focused on luminescence of trivalent rare earth ions in phosphates, tungstates, borates, molybdates, and aluminates, among which rare earth doped borates are especially attractive because of their wide UV transparency, exceptional optical damage thresholds, excellent chemical and thermal stability, and high luminescence efficiency [24–34]. The luminescence study of a series of such compounds provides much valuable information for optical applications.

It is our main interest to synthesize another family of newly developed Sm^{3+} doped phosphors via low temperature initiated combustion process and investigate their photoluminescence properties in view of the commercial importance of reddish-orange color emitting phosphors. Generally, the typical Sm-activated phosphors usually show charge-transfer absorption of Sm^{3+} –O^{2-} interaction in the UV region. However, there was no obvious charge-transfer

absorption of Sm^{3+}– O^{2-} interaction or host absorption band that could be detected in the excitation spectrum. Only direct excitation of Sm^{3+} ions could be observed. It is recognized that Sm^{3+} interaction with the host lattice is very weak, and no energy transfer occurs between Sm^{3+} and host. The reddish orange light of Sm^{3+} consists of three emission peaks in the visible region near 563, 595, and 641 nm, which are assigned to the intra-4f-shell transitions from the excited level $^4G_{5/2}$ to ground levels $^6H_{5/2}$, $^6H_{7/2}$, $^6H_{9/2}$, respectively.

As we know different material preparation methods have some important effects on material microstructure and physical properties. The combustion method provides an interesting alternative over other elaborated techniques because it offers several attractive advantages such as: simplicity of experimental set-up; surprisingly short time between the preparation of reactants and the availability of the final product; and being cheap due to energy saving.

The main aim of the combustion method is the rapid decomposition of the rare earth nitrate in the presence of an organic fuel. During the reaction, many gases, such as CO_2, N_2, NO_2 and H_2O, as well as a large amount of heat are released in a short period of time before the process terminates with white, foamy and crispy products. Many times final products are found to be composed of nanosized particles. This work has been carried out with the aim to prepare ,compare and investigate the high intensity photoluminescence nanosized crystalline powders of $LaAlO_3$ doped with Sm^{3+} and co-doped with some monovalent metal ions [Li^+, Na^+, K^+, Ag^+] sintered at 1000ºC temperature.

A series of $La_{1-x}Sm_xAlO_3$ phosphor have been synthesized with the dopant concentration ranging from 01 to 20 mol%. The crystalline structure and morphology of prepared nano-materials have also been discussed. The crystalline structure of prepared materials, morphology of particles and their photoluminescence properties are characterized by XRD, SEM and PL spectra with 245 nm lasers for excitation.

2. Experimental

High purity chemicals $La(NO_3)_3$, $Al(NO_3)_3$ [1.0mole], $Sm(NO_3)_3$,,$LiNO_3$, $NaNO_3$, KNO_3 $AgNO_3$ in such a way that total La^{3+} + [Sm^{3+} + M^+] = 1.0 mole, and carbohydrazide as a fuel were used to prepare Sm^{3+} doped nano crystals with general formula $La_{(1-x)}AlO_3$ **:** Sm_x^{3+} & where x is 1 to 18 mol%, $La_{(1-x+y)}AlO_3$ **:** Sm_x^{3+}, M_y^+ where y is 0.5 to 1 mol% , by heating rapidly an aqueous concentrated paste in a preheated furnace maintained at 600,700, and 1000 ^{0}C to improve the crystallinity of the materials. The structure and morphology of materials have been examined by X-ray diffraction and scanning electron microscopy. XRD results reveal that the sample begins to crystallize at 600°C , and pure $LaAlO_3$ phase can be obtained at 700°C. The stoichiometric amount of the fuel was calculated by using total oxidizing and reducing valences [35]. The paste was made by dissolving metal nitrates and fuel in a minimum amount of doubly distilled water. In furnace, the material had rapid dehydration followed by decomposition, generating combustible gases which burnt with a flame and producing a white solid. The solid thus obtained was again fired at 1000°C for 3h to increase the crystallinity. Finally the powder was characterized by XRD, SEM, PL measurement to check the crystallinity, particles size and luminescence intensity of the phosphor respectively.

3. Characterization & Discussion

3.1 XRD studies

The structural characterizations of compounds were done on XRD diffractometer (Rigaku Ultima IV) using Cu Kα radiation (1.541841 Å).

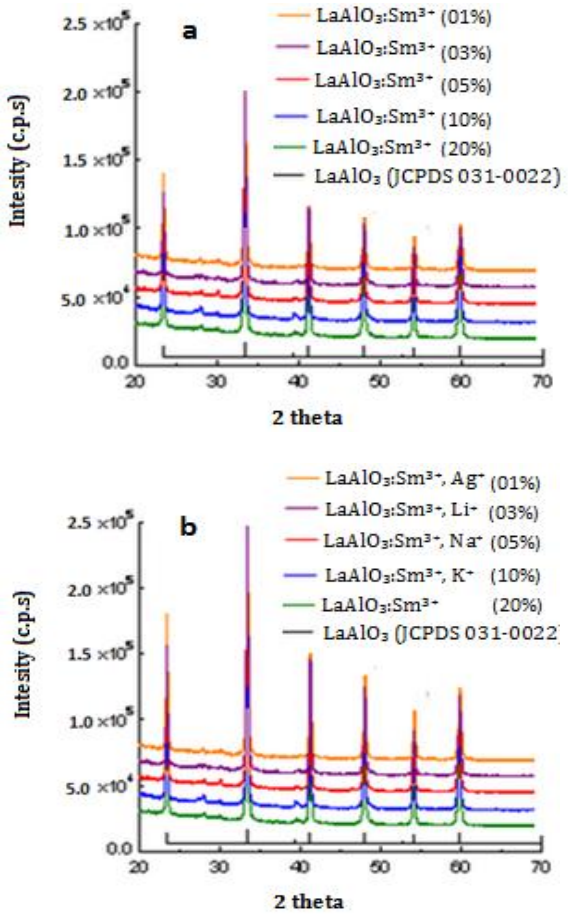

Figure1: XRD spectra of **(a)** $LaAlO_3$:Sm^{3+} **(b)** $LaAlO_3$:Sm^{3+} [Li^+, Na^+, K^+, Ag^+] phosphors showing sharp xrd peaks.

The structural characterizations of compounds were done on XRD diffractometer (Rigaku Ultima IV) using Cu Kα radiation**.** XRD results reveal that the sample begins to crystallize at 600°C , and pure $LaAlO_3$ phase can be obtained at 700°C . Crystallinity, particle size, and surface roughness of the phosphor materials have strong effects on the photoluminescence. Fig1.(a & b) showed the X-ray diffractograms of Sm^{3+} doped $LaAlO_3$ $LaAlO_3$:Sm^{3+} [Li^+, Na^+, K^+, Ag^+] phosphors . The phase analysis demonstrated (Fig.1) that $LaAlO_3$:Sm^{3+} belongs to trigonal crystal system with R3m (160) space group having unit cell dimensions: *a* =b = 5.364 Å and *c* = 13.11 Å. This was in good agreement with the standard JCPDS C. NO. 031-0022. In this phosphor, trivalent lanthanum ions were replaced by trivalent samarium ions. Dopant ions (Sm^{3+}) concentration variation from 1mol % to 20 mol% have no noticeable effect on the obtained X-ray diffractograms of the as-prepared

$LaAlO_3:Sm^{3+}$ phosphors, indicating that the doped ions were occupied the primordial La^{3+} sites of the $LaAlO_3$ lattice**.** All measurements were carried out at room temperature. The structural characterization was done by a high resolution X-ray diffraction (XRD) using a Rigaku Ultima IV diffractometer in the θ–2θ configuration and using Cu Kα radiation (1.5418 Å) using Scherrer equation (1).

$$\tau = K\lambda / \beta \cos\theta \quad (1)$$

where

- τ is the mean size of the ordered (crystalline) domains, which may be smaller or equal to the grain size;
- K is a dimensionless shape factor, with a value close to unity. The shape factor has a typical value of about 0.9, but varies with the actual shape of the crystallite;
- λ is the X-ray wavelength;
- β is the line broadening at half the maximum intensity (FWHM), after subtracting the instrumental line broadening, in radians. This quantity is sometimes denoted as *(2θ)*;
- θ is the Bragg angle was used to calculate the crystallite size of all materials.

At least five prominent peaks from each XRD (samples with various Sm^{3+} concentration) were used for calculation and peaks belonging to different phases were also taken into consideration. Maximum and minimum values obtained for each type of lattice are reported as range of crystallite size (e.g. 40±5nm for $LaAlO_3$).

3.2 SEM micrograph and particle size analysis

The SEM micrographs were obtained by JEOL JSM6300 scanning electron microscope. SEM images indicate that the Sm^{3+} - doped $LaAlO_3$ phosphors are composed of aggregated spherical particles with sizes ranging from 40±5 to 80±5nm. Figures 2 (a to d) exhibited the surface morphologies of $LaAlO_3$, $LaAlO_3:Sm^{3+}$ and $LaAlO_3:Sm^{3+}$, [Li^+, Na^+, K^+, Ag^+] particles. Generally non- uniformity of shape and size is associated with the non-uniform distribution of temperature and mass flow in the combustion flame. However the SEM images of $LaAlO_2:Sm^{3+}$ particles (fig. 2a,b) show small and coagulated particles of nearly cubical shape with larger size distribution. The surface morphology of $LaAlO_2:Sm^{3+}$ lattices as depicted in the picture 2a and 2b is smooth and aggregated spherical particles of different sizes are observed.

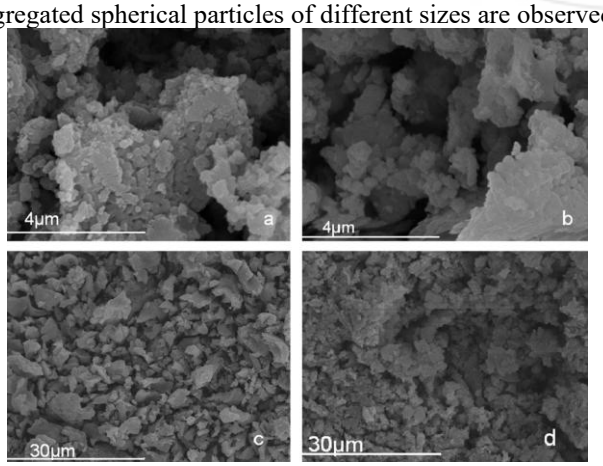

Figure 2: SEM micrographs of phosphor particles (a,b,c,d,): (a) $LaAlO_3$ lattice (b) $LaAlO_3:Sm^{3+}$ (c) $LaAlO_3:Sm^{3+}$,[Li^+] (d) $LaAlO_3:Sm^{3+}$,[Na^+]

The smooth surface of phosphor can reduce the non-radiation and scattering, thus beneficial to the luminescence efficiency in application[36-37]. The dence packed small particles can prevent the phosphor from aging.

3.3 Photoluminescence Properties

For the photoluminescence measurement, 0.05g powder samples were pressed into pellets and then exposed to a He–Cd laser (245nm) with an optical power of 30mW for excitation. The emitted light was analyzed by HR-4000 Ocean Optics USB spectrometer optimized for the UV–vis range. Under the excitation of UV light (245nm) and low-voltage electron beams (1–3kV) , the Sm^{3+} -doped LaAlO3 phosphors show the characteristic emissions of the Sm^{3+} ($^4G_{5/2}\rightarrow{}^6H_{5/2}$, $^6H_{7/2}$, $^6H_{9/2}$ transitions) with a strongest Yellow, Yellow-orange & Orange-red color. The room-temperature emission spectra of Sm^{3+} doped $LaAlO_3$ crystals with different doping concentrations are shown in figures 3 (a to b). The emission spectra were obtained by monitoring at 245nm under an excitation of ultraviolet light. The obtained products emitted the red luminescence of varying intensities, which showed the activator Sm^{3+} & co-activator Li^+, Na^+, K^+, Ag^+ , had successfully entered the host lattice of $LaAlO_3$. The characteristic emissions of phosphor consist of five emission peaks, which are attributed to the transitions from $^4G_{5/2}$ state to ^6H_J (J=5/2, 7/2, 9/2, 11/2,13/2) states of Sm^{3+} ions . Among these, emission peak located at 562-577, 598, 617-619, 653-655, 708-709, are attributed to the transitions of $^4G_{5/2}\rightarrow{}^6H_{5/2}$, $^4G_{5/2}\rightarrow{}^6H_{7/2}$, $^4G_{5/2}\rightarrow{}^6H_{9/2}$, $^4G_{5/2}\rightarrow{}^6H_{11/2}$ and $^4G_{5/2}\rightarrow{}^6H_{13/2}$, respectively [38–42]. Among these emission peaks, the transition emission $^4G_{5/2}\rightarrow{}^6H_{7/2}$ (565nm, strongest yellow, a strong Yellow-orange located at 598nm & 611 nm for orange-red color due to the $^4G_{5/2}\rightarrow{}^6H_{J=5/2\,,\,7/2\,,\,9/2}$ magnetic dipole transition of Sm^{3+} ion having a magnetic dipole (MD) allowed one and also a electric dipole (ED) dominated one and the other transition $^4G_{5/2}\rightarrow{}^6H_{J=11/2\,,13/2}$ (653 nm, 708-709nm, red) is purely an ED one. The MD transition does not appreciably depend on the chemical surroundings of the luminescent center and its symmetry; however, the ED transition belongs to hypersensitive transitions. Generally, the intensity ratio of ED to MD transitions has been used to evaluate the symmetry of the local environment of the trivalent 4f ions. The greater the intensity of the ED transition, the more the asymmetry nature [43]. The exact positions of emission peaks in various lattices are shown in table 1. The $^4G_{5/2}\rightarrow{}^6H_{J=5/2\,,\,7/2\,,\,9/2}$ transition is well known to be mainly a magnetic dipole transition when the Sm^{3+} ions locate in a high symmetric position while the $^4G_{5/2}\rightarrow{}^6H_{J=11/2\,,13/2}$ transitions are essentially electric dipole transitions which appear only when Sm^{3+} ion locates at sites without inversion symmetry [44-45]. In fig 3, the emission intensity of all peaks increased with increase of doping concentration from 1% to 3 mol % and then starts decreasing. It becomes nearly one fifth with 20 mol% doping of Sm^{3+} in $LaAlO_3:Sm^{3+}$ phosphors. The emission and decay behaviors of the $^4G_{5/2}\rightarrow{}^6H_{7/2}$ transition depend on the concentration of Sm^{3+} ions. The emission intensity increases with Sm^{3+} concentration up to 3 mol%, and then decreases quickly. The decay time also begins to decrease rapidly at around 3 mol%.

At higher concentrations (x> 0.03), however, the observed decay were non-radiative, and the non-radiative change becomes more prominent as (Sm^{3+}) content increases, revealing that more than one relaxation process exists.

Table 1: The emission peaks in $LaAlO_3:Sm^{3+}$, [Li^+, Na^+, K^+, Ag^+] nano-phosphors

Lattice	$^4G_{5/2}\rightarrow{}^6H_{5/2}$ **Yellow** (nm) **Strongest peak**	$^4G_{5/2}\rightarrow{}^6H_{7/2}$ & $^4G_{5/2}\rightarrow{}^6H_{9/2}$ Orange-**Yellow** & Orange-**Red** (nm) **Strong**	$^4G_{5/2}\rightarrow{}^6H_{11/2}$ & $^4G_{5/2}\rightarrow{}^6H_{13/2}$ **Red** (nm) Weak peak
$La_{0.94}Sm_{0.05}K_{0.01}AlO_3$	577	**598 & 611**	653 & 709
$La_{0.96}Sm_{0.03}Na_{0.01}AlO_3$	**565**	598,619,625	655 655,708
$La_{0.89}Sm_{0.10}Li_{0.01}AlO_3$	565	599 ,617,625	654, 708
$La_{0.80}Sm_{0.18}Ag_{0.02}AlO_3$	575	598,617,	654,708

It is expected that with the increase of Sm^{3+} ions, photoluminescence should increase. However, the emission intensity tends to decrease above 3 mol% of Sm^{3+} ions due to concentration quenching, because of non-radiative interaction between ions as the resonant energy transfer becomes stronger. As the concentration is increased, the Sm^{3+} ions are packed closer and closer together, which favors the transfer of energy from one Samarium ion to the next by a resonance process; the energy eventually reaches a sink from which it is dissipated by non-radiative processes rather than by the emission of visible light [46-47]. In the present case, the emission spectrum shows three strong sharp peaks at the 565, 598nm and 611nm corresponding to the magnetic dipole transition ($^4G_{5/2}\rightarrow{}^6H_{J=5/2\,,\,7/2\,,\,9/2}$) and electric dipole transition ($^4G_{5/2}\rightarrow{}^6H_{J=5/2\,,\,7/2\,,\,9/2}$) of Sm^{3+} emission respectively. Other weak intensity peaks are seen on right side of these three strong peaks. It may be mentioned that similar results from magnetic dipole transition ($^4G_{5/2}\rightarrow{}^6H_{J=5/2\,,\,7/2\,,\,9/2}$) were observed for Sm^{3+} doped $LaAlO_3$ host [48] and the strong yellow, yellow-orange & orange-red emission of the prepared $LaAlO_3:Sm^{3+}$, [Li^+, Na^+, K^+, Ag^+] nano-phosphors had already not been proposed for its probable utility for display applications. Earlier workers observed these peaks only in the Sm^{3+} doped $LaAlO_3$ host which substantiate the presence of Sm^{3+} ions [48-49]. The intensity ratio of 598 nm peak to 611 nm peak is a measure of asymmetry of the Sm^{3+} site in the host lattice [50].

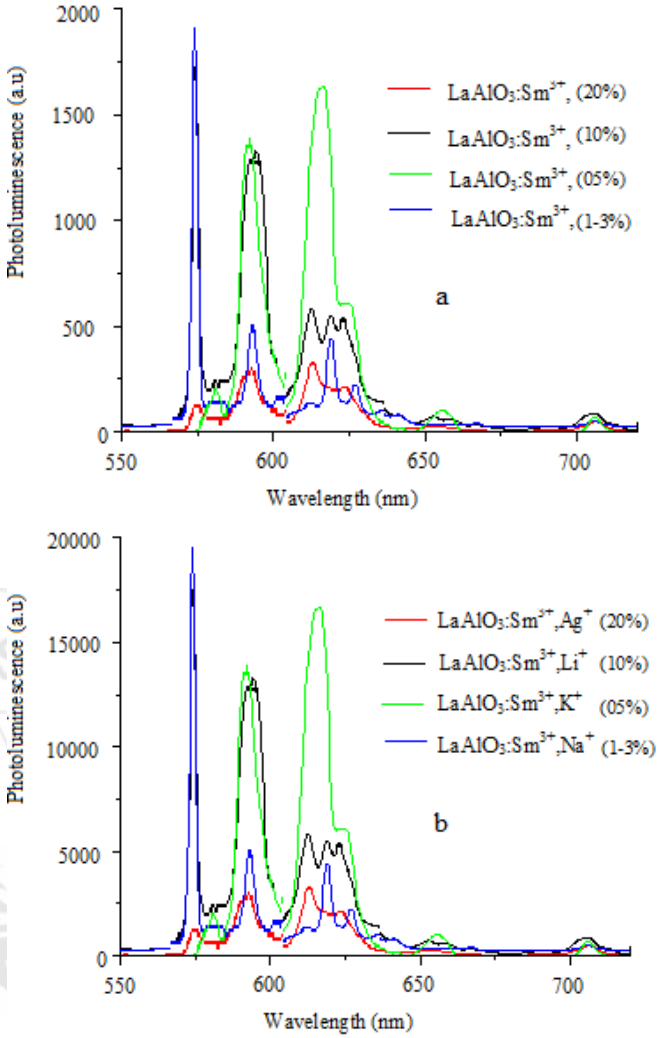

Figure 3: PL spectra of **(a)** $LaAlO_3:Sm^{3+}$ **(b)** $LaAlO_3:Sm^{3+}$ [Li^+, Na^+, K^+, Ag^+] phosphors showing enhanced yellow, orangish-yellow & orangish-red emission.

Luminescence study shows that magnetic dipole transition ($^4G_{5/2}\rightarrow{}^6H_{J=5/2\,,\,7/2\,,\,9/2}$) is prominent over the other electric dipole transition ($^4G_{5/2}\rightarrow{}^6H_{J=11/2\,13/2}$), which is attributed to occupancy of inversion symmetry site by more Sm^{3+} ions in Sm^{3+} doped $LaAlO_3$. If more Sm^{3+} ions have occupancy at the inversion site, the emission intensity from the ($^4G_{5/2}\rightarrow{}^6H_{J=5/2\,,\,7/2\,,\,9/2}$) transition will enhance and the phosphor will primarily exhibit orange luminescence. In the present investigation, the intensity of ($^4G_{5/2}\rightarrow{}^6H_{J=5/2\,,\,7/2\,,\,9/2}$) transition is comparable to the intensity of other electric dipole transition ($^4G_{5/2}\rightarrow{}^6H_{J=11/2\,,\,13/2}$). Effect of co-doping of Li^+, Na^+ , K^+ & Ag^+ ions on $LaAlO_3$: Sm^{3+} structure had been investigated to study the photoluminescent behavior of this lattice. There is no significant effect on the structure of $LaAlO_3:Sm^{3+}$ co-doped with monovalent ions [Li^+, Na^+, K^+, Ag^+] as the ionic radii of Sm^{3+} , Na^+ & Ag^+ correspond to 95.8 pm ,102 pm & 115 pm respectively are not much different from that of La^{3+} (103.7 pm), therefore these ions are likely to substitute for La^{3+} ion and act as the luminescence centers [51]. But Li^+ ions and K^+ ions have ionic radii 76 and 138nm respectively having a large difference, are also incorporated in $LaAlO_3$ lattice successfully, due to this difference of ionic radii of Li^+ and K^+ ions , the $LaAlO_3$ lattice had slight deformations which

lead to the variation in the heights of diffraction peaks in their patterns. As the ionic radius of Li^+ ion is less, there is a possibility of some of the ions to reside in interstitial sites between or among the host ions. For Na^+ ions [102pm], they could be located at La^{3+} [103.7pm] sites more easily than for K^+ ions [138pm] because of their bigger ionic radii than La^{3+} [103.7pm]. In fig.1, note that the XRD diffractogram of $LaAlO_3$: Sm^{3+} nano - material co-doped with Li^+, Na^+, K^+ & Ag^+ ions were obviously almost identical but the relative intensities of crystal faces (111), (200) and (221) were different from each other. We think this observation can be assigned to the enormous changes in lattice constants of these samples. The corresponding unit-cell constants and unit cell volumes of cubic $LaAlO_3$: Sm^{3+} samples as well as doped with Li^+, Na^+, K^+ & Ag^+ are calculated from the distance between the adjacent (200) planes corresponding to diffraction peaks nearly $2\theta = 37.30^0 \pm 4$ and are listed in Table 2.

Table2: The calculated lattice parameters of $LaAlO_3$: Sm^{3+} co-doped with Li^+, Na^+, K^+ & Ag^+ ions

Phosphors	*2θ*	*hkl/200*	*a (A)*	*V (A^3)*
$LaAlO_3$:Sm^{3+}	37.342^0	2.4061	4.8121	111.434
$LaAlO_3$:Sm^{3+},Li^+	37.283^0	2.4098	4.8197	111.964
$LaAlO_3$:Sm^{3+},Na^+	37.274^0	2.4101	4.8203	112.014
$LaAlO_3$:Sm^{3+},A^+	37.271	2.4102	4.8201	112.013
$LaAlO_3$:Sm^{3+}, K^+	37.257^0	2.4114	4.8227	112.175

It is noticed that if the ions with larger radius substitute the smaller cations in the crystalline lattice, the cell volume of the host compound is increased [53]. Therefore, as shown in Table 2, the cell volumes of $LaAlO_3$: Sm^{3+} after co-doping with Na^+, Ag^+ and K^+ ions increased, because the ionic radii of Na^+ ions (102 pm), Ag^+ (115pm) and K^+ ions (138 pm) are larger than that of La^{3+} ions (100 pm). The cell volume should decrease with the co-doping of Li^+ ions, but the cell volume of $LaAlO_3$: Sm^{3+} co-doped with Li^+ ions increased, despite the fact that the Li^+ is smaller than La^{3+}. This increase may be due to the larger size of Li^+ ions than that of interstitial sites. We observed a remarkable improvement in the luminescence intensity of all emission peaks from Sm^{3+} particularly for $^4G_{5/2} \rightarrow {}^6H_{J=5/2\,,\,7/2\,,\,9/2}$) transition at 565, 598 and 611nm when the $LaAlO_3$ lattices is co-doped with monovalent ions [Li^+, Na^+, K^+, Ag^+] . There is an increase of about 10, 20 and 400 % respectively in the luminescence intensity when monovalent ions [Li^+, Na^+, K^+, Ag^+] are co-doped (fig.3 b). It seems that the co-doping of mono-valent ions increased the improved energy transfer from La^{3+} to Sm^{3+} and creating the oxygen vacancies which act as sensitizers [52] and facilitate the strong mixing of the La-O and Sm-O charge transfer states, and thus promote energy migration from the La-O CTS (charge transfer state) to Sm^{3+}. Further, more are the oxygen vacancies generated by co-doping of monovalent ions; more is the effective energy transfer between La^{2+} and Sm^{3+} ions. Finally, it can be concluded that the large increase in the emission intensity of the $^4G_{5/2} \rightarrow {}^6H_{J=5/2\,,\,7/2\,,\,9/2}$) transition at 565, 598 and 611nm is due to improved energy transfer and reduced symmetrical environment around Sm^{3+} when co-doped with monovalent ions [Li^+, Na^+, K^+, Ag^+] & co-doping had different effects on energy transfer ($K^+ > Li^+ > Ag^+ > Na^+$), which is in accordance with the sequence of luminescence from $^4G_{5/2} \rightarrow {}^6H_{J=5/2\,,\,7/2\,,\,9/2}$ transition of the Sm^{3+}. In a similar case [53], the enhancement of Sm^{3+} luminescence intensity with the co-doping of alkali metals ions in Sr_2CeO_4 host lattice is due to the generation of oxygen vacancies to promote the energy transfer from Ce^{4+} to Sm^{3+}, reduce environment symmetry around Sm^{3+} ions and cause hole traps to quench the Ce-O CTS luminescence.

4. Conclusion

$LaAlO_3$:Sm^{3+}, [Li^+, Na^+, K^+, Ag^+] nano-phosphors with varying dopant concentrations of Sm^{3+} from 1 to 20 mol% & codopants concentration of [Li^+, Na^+, K^+, Ag^+] is 0.5 to 1 mol% were prepared by combustion synthesis method and the samples were further heated to 600,700, and 1000 ^{0}C to improve the crystallinity of the materials. The structure and morphology of materials have been examined by X-ray diffraction and scanning electron microscopy. XRD results reveal that the sample begins to crystallize at 600°C , and pure $LaAlO_3$ phase can be obtained at 700°C. SEM images indicate that the Sm^{3+} -doped LaAlO3 phosphors are composed of aggregated spherical particles with sizes ranging from 40 to 80nm . Under the excitation of UV light (245nm) and low-voltage electron beams (1–3kV) , the Sm^{3+} -doped $LaAlO_3$ phosphors show the characteristic emissions of phosphor consist of five emission peaks, which are attributed to the transitions from $^4G_{5/2}$ state to ^6H_J (J=5/2, 7/2, 9/2, 11/2 ,13/2) states of Sm^{3+} ions with Yellow, Yellow-orange and Orange-red color. Among these, emission peak located at 565, 598, 611, 653, 708 nm are attributed to the transitions of $^4G_{5/2} \rightarrow {}^6H_{5/2}$, $^4G_{5/2} \rightarrow {}^6H_{7/2}$, $^4G_{5/2} \rightarrow {}^6H_{9/2}$, $^4G_{5/2} \rightarrow {}^6H_{11/2}$ & $^4G_{5/2} \rightarrow {}^6H_{13/2}$ respectively. Among these emission peaks, the transition emission $^4G_{5/2} \rightarrow {}^6H_J$ (J=5/2, 7/2, 9/2) for peak at 563, 598, 611nm is strongest for Yellow, orangish-Yellow and strong orangish-Red emission repectively is due to the magnetic dipole transition of Sm^{3+} ion having a magnetic dipole (MD) allowed one and also an electric dipole (ED) dominated one but the other weak transition $^4G_{5/2} \rightarrow {}^6H_{11/2}$ & $^4G_{5/2} \rightarrow {}^6H_{13/2}$ (653 nm, 708nm red) is purely an ED one. Highest photoluminescence intensity is observed with 3 mol% doping of Sm^{3+} i.e. (Sm^{3+}+ Na^+=3mol% for promising Yellow) (Sm^{3+}+ K^+=3mol%, for Yellow-orangish & Orangish-red) , made $LaAlO_3$:Sm^{3+}, [Li^+, Na^+, K^+, Ag^+] a strong competitor for promising Yellow, Yellow-orange & also for Orange-red colored display applications.

Finally, it can be concluded that the large increase in the luminescence intensity of the $^4G_{5/2} \rightarrow {}^6H_J$ (J=5/2, 7/2, 9/2) transitions is due to improved energy transfer and reduced symmetrical environment around Sm^{3+} when monovalent ions [Li^+, Na^+, K^+ , Ag^+] are co-doped & co-doping had different effects on energy transfer ($K^+ > Li^+ > Ag^+ > Na^+$), which is in accordance with the sequence of luminescence from $^4G_{5/2} \rightarrow {}^6H_J$ (J=5/2, 7/2, 9/2) transition of the Sm^{3+}. The $LaAlO_3$:Sm^{3+} [K^+] nano-material showing very high yellow-orange & orange-red luminescence of nearly at 598nm and red at 611 nm is definitely a material for further investigation for its use in yellow-orange- red color and the $LaAlO_3$:Sm^{3+} [Na^+] i.e. (Sm^{3+}+ Na^+=3mol%) for promising Yellow displays applications. It must be noted that this research work resulting from magnetic dipole transition

($^4G_{5/2} \rightarrow {}^6H_{J=5/2\,,\,7/2\,,\,9/2}$) for Sm^{3+} doped $LaAlO_3$ host [48] and the strong yellow, yellow-orange & orange-red emission of the prepared $LaAlO_3:Sm^{3+}$, [Li^+, Na^+, K^+, Ag^+] nano-phosphors had already not been proposed for its probable utility for display applications. So in this way this phosphor became more attractive for further research work.

5. Acknowledgments

This nano-phosphor had been prepared in Inorganic Lab no 218, Deptt. of Chemistry , M.D.U Rohtak-124001, Haryana, India. by Dr. Subhash Chand Chopra, under supervision of Senior Professor Ishwar Singh, Pro-Vice Chancellor, P.D.M University , Bahadurgarh-124507, Haryana, India. & with support of Professor V.K. Sharma, H.O.D Chemistry, Department of Chemistry, M.D.U Rohtak.

References

[1] C. Duan, J. Yuan, X. Yang, J. Zhao, Y. Fu, G. Zhang, Z. Qi, Z. Shi, J. Phys. D: Appl. Phys. 38 (2005) 3576.
[2] A. Komeno, K. Uematsu, K. Toda, M. Sato, J. Alloys Compd. 408–412 (2006) 871.
[3] A.H. Kitai, Thin Solid Films 445 (2003) 367.
[4] V. Sivakumar, U.V. Vardaraju, J. Electrochem. Soc. 152 (10) (2005) H168.
[5] O. V. Solovyev, and B. Z. Malkin,"Modeling of electron-vibrational $4f^n$–$4f^{n-1}$ ^{1}5d spectra in $LiYF_4:RE^{3+}$ crystals," Journal of Molecular Structure, 838, pp. 176-181, 2007.
[6] K. Ogasawara, S. Watanabe, H. Toyoshima, M.G. Brik, "Handbook on Physics and Chemistry of Earths", **37**, pp.1-59, 2007.
[7] C. Shi, J. Shi, J. Deng, Z. Han, Y. Zhou, G. Zhang, *J. Electron Spectrosc. Phenom.,* **79**, 121,1996
[8] C. Feldmann, T. Justel, C.R. Ronda, P.J. Schmidt, Adv. Funct. Matter 13 (7) (2003) 511.
[9] J.E. Hubeey, Inorganic Chemistry: Principles of Structure and Reactivity, 2nd ed., Harper and Row Publisher Inc., New York, 1978.
[10] N. S. Hussain, G. Hungerford, R. El-Mallawany et al., "Absorption and emission analysis of RE3+(Sm3+ and Dy3+): Lithium boro tellurite glasses," Journal of Nanoscience and Nanotechnology, vol. 9, no. 6, pp. 3672–3677, 2009.
[11] M. D. Que, Z. P. Ci, Y. H. Wang, G. Zhu, Y. R. Shi, and S. Y. Xin, "Synthesis and luminescent properties of Ca2La8(GeO4)6O2:RE3+ (RE3+=Sm3+, Tb3+, Dy3+, Sm3+, Tm3+) phosphors," Journal of Luminescence, vol. 144, pp. 64–68, 2013.
[12] A. Tang, D. F. Zhang, and L. Yang, "Photoluminescence characterization of a novel red-emitting phosphor In2(MoO4)3:Sm3+ for white light emitting diodes," Journal of Luminescence, vol. 132, no. 6, pp. 1489–1492, 2012.
[13] S. A. Naidu, S. Boudin, U. V. Varadaraju, and B. Raveau, "Sm3+ and Tb3+ emission in molybdenophosphate Na2Y(MoO4)(PO4)," Journal of the Electrochemical Society, vol. 159, no. 4, pp. J122–J126, 2012. View at Publisher ·
[14] [14] X. L. Dong, J. H. Zhang, X. Zhang, Z. D. Hao, and S. Z. Lv, "Synthesis and photoluminescence properties of Sm2+ doped Sr9Sc(PO4)7 phosphors for white light-emitting diodes," Ceramics International, vol. 40, no. 4, pp. 5421–5423, 2014.
[15] [15] P. Abdul Azeem, M. Kalidasan, R. R. Reddy, and K. Ramagopal, "Spectroscopic investigations on Tb3 doped lead fluoroborate glasses," Optics Communications, vol. 285, no. 18, pp. 3787–3791, 2012.
[16] [16] E. Cavalli, P. Boutinaud, R. Mahiou, M. Bettinelli, and P. Dorenbos, "Luminescence dynamics in Tb3+-doped CaWO4 and CaMoO4 crystals," Inorganic Chemistry, vol. 49, no. 11, pp. 4916–4921, 2010.
[17] [17] A. Boukhris, M. Hidouri, B. GloriSmx, and M. Ben Amara, "Correlation between structure and photoluminescence of the Smropium doped glaserite-type phosphate Na2SrMg(PO4)2," Materials Chemistry and Physics, vol. 137, no. 1, pp. 26–33, 2012.
[18] [18] Y. Zhang, C. H. Lu, L. Y. Sun, Z. Z. Xu, and Y. R. Ni, "Influence of Sm2O3 on the crystallization and luminescence properties of boroaluminosilicate glasses," Materials Research Bulletin, vol. 44, pp. 179–183, 2009.
[19] [19] M. Sobczyk, P. Starynowicz, R. Lisiecki, and W. Ryba-Romanowski, "Synthesis, optical spectra and radiative properties of Sm2O3:PbO:P2O5 glass materials," Optical Materials, vol. 30, no. 10, pp. 1571–1575, 2008.
[20] [20] V. Venkatramu, P. Babu, C. K. Jayasankar, T. Tröster, W. Sievers, and G. Wortmann, "Optical spectroscopy of Sm3+ ions in phosphate and fluorophosphate glasses," Optical Materials, vol. 29, no. 11, pp. 1429–1439, 2007.
[21] [21] S. Nishiura, S. Tanabe, K. Fujioka, and Y. Fujimoto, "Properties of transparent Ce:YAG ceramic phosphors for white LED," Optical Materials, vol. 33, no. 5, pp. 688–691, 2011.
[22] [22] X. M. Zhang and H. J. Seo, "Luminescence properties of novel Sm3+, Dy3+ doped LaMoBO6 phosphors," Journal of Alloys and Compounds, vol. 509, pp. 2007–2010, 2011.
[23] [23] A. M. Pires, M. F. Santos, M. R. Davolos, and E. B. Stucchi, "The effect of Sm3+ ion doping concentration in Gd2O3 fine spherical particles," Journal of Alloys and Compounds, vol. 344, no. 1-2, pp. 276–279, 2002.
[24] [24] K. Driesen, V. K. Tikhomirov, and C. Gorller-Walrand, "Sm3+ as a probe for rare-earth dopant site structure in nano-glass-ceramics," Journal of Applied Physics, vol. 102, Article ID 024312, 2007.
[25] [25] C. H. Yan, L. D. Sun, C. S. Liao et al., "Sm3+ ion as fluorescent probe for detecting the surface effect in nanocrystals," Applied Physics Letters, vol. 82, no. 20, pp. 3511–3513, 2003.
[26] [26] R. Stefani, A. D. Maia, E. E. S. Teotonio, M. A. F. Monteiro, M. C. F. C. Felinto, and H. F. Brito, "Photoluminescent behavior of SrB4O7:RE2+ (RE=Sm and Sm) prepared by Pechini, combustion and ceramic methods," Journal of Solid State Chemistry, vol. 179, no. 4, pp. 1086–1092, 2006.
[27] [27] Y. Won, H. Jang, W. Im, D. Jeon, and J. Lee, "Red-emitting LiLa2O2BO3: Sm3+, Sm3+ phosphor for

near-ultraviolet light-emitting diodes-based solid-state lighting," Journal of The Electrochemical Society, vol. 155, no. 9, pp. J226–J229, 2008.
[28] M. Ayvacıklı, A. Ege, and N. Can, "Radioluminescence of SrAl2O 4:Ln3+ (Ln = Sm, Sm, Dy) phosphor ceramic," Optical Materials, vol. 34, no. 1, pp. 138–142, 2011.
[29] Y. M. Yang, Z. Y. Ren, Y. C. Tao, Y. M. Cui, and H. Yang, "Sm3+ emission in SrAl2B2O7 based phosphors," Current Applied Physics, vol. 9, pp. 611–621, 2009.
[30] D. Tu, Y. J. Liang, R. Liu, Z. Cheng, F. Yang, and W. L. Yang, "Photoluminescent properties of LiSrxBa1−xPO4:RE3+ (RE = Sm3+, Sm3+) f–f transition phosphors," Journal of Alloys and Compounds, vol. 509, no. 18, pp. 5596–5599, 2011.
[31] J. H. Hao, J. Gao, and M. Cocivera, "Tuning of the blue emission from Smropium-doped alkaline earth chloroborate thin films activated in air," Applied Physics Letters, vol. 82, no. 17, pp. 2778–2780, 2003.
[32] A. E. Henkes and R. E. Schaak, "Synthesis of nanocrystalline REBO3 (RE=Y, Nd, Sm, Sm, Gd, Ho) and YBO3:Sm using a borohydride-based solution precursor route," Journal of Solid State Chemistry, vol. 181, no. 12, pp. 3264–3268, 2008.
[33] G. F. Ju, Y. H. Hu, H. Y. Wu et al., "A red-emitting heavy doped phosphor Li6Y(BO3)3:Sm3+ for white light-emitting diodes," Optical Materials, vol. 33, pp. 1297–1301, 2011.
[34] J. Yang, C. M. Zhang, C. X. Li, Y. G. Yu, and J. Lin, "Energy transfer and tunable luminescence properties of Sm3+ in TbBO3 microspheres via a facile hydrothermal process," Inorganic Chemistry, vol. 47, no. 16, pp. 7262–7270, 2008.
[35] S. Ekambaram, K. Patil, *J. Alloys Compd*., **248,** 7,1997.
[36] Y. Conga, B. Lia, B. Leia, X. Wanga, C. Liua, J. Liua, W. Li, J Lumin, 128, 2008, 105.
[37] G. Liu, G. Hong, J. Wang, X. Dong, *J. Alloys Compd*., **432**, 200, 2007.
[38] F. He, P. Yang, D. Wang et al., "Hydrothermal synthesis, dimension evolution and luminescence properties of tetragonal LaVO4:Ln (Ln = Sm3+, Dy3+, Sm3+) nanocrystals," Dalton Transactions, vol. 40, no. 41, pp. 11023–11030, 2011.
[39] G. S. R. Raju, J. Y. Park, H. C. Jung et al., "Excitation induced efficient luminescent properties of nanocrystalline Tb3+/Sm3+:Ca2Gd8Si6O26 phosphors," Journal of Materials Chemistry, vol. 21, no. 17, pp. 6136–6139, 2011.
[40] X. Lin, X. S. Qiao, and X. P. Fan, "Synthesis and luminescence properties of a novel red SrMoO4:Sm3+,R+phosphor," Solid State Sciences, vol. 13, no. 3, pp. 579–583, 2011.
[41] Z. Yang, Z. Zhao, M. Que, and Y. Wang, "Photoluminescence and thermal stability of β-SiAlON:Re (Re = Sm, Dy) phosphors," Optical Materials, vol. 35, no. 7, pp. 1348–1351, 2013.
[42] M. Puchalska and E. Zych, "The effect of charge compensation by means of Na+ ions on the luminescence behavior of Sm3+-doped CaAl4O7 phosphor," Journal of Luminescence, vol. 132, no. 3, pp. 826–831, 2012.
[43] G. Lakshminarayana, R. Yang, J. R. Qiu, M. G. Brik, G. A. Kumar, and I. V. Kityk, "White light emission from Sm3+/Tb3+ codoped oxyfluoride aluminosilicate glasses under UV light excitation," Journal of Physics D: Applied Physics, vol. 42, no. 1, , 2009.
[44] R. Ningthoujam, V. Sudarsan, S. Kulshreshtha, *J. Lumin*., **127** , 747,2007.
[45] X. Gao, L. Lei, C. Lv, Y. Sun, H. Zheng, Y. Cui., *J. Solid* State Chem., **181**, p.1776, 2008.
[46] E. Perea, M. Estrada, M. Gracia, *J. Phys.,* **31** , 7,1998.
[47] T. Hayakawa, N. Kamt, K. Yamada, *J. Luminesc*., **68**, 179, 1996.
[48] P. Deren, J. Krupa, *J. Lumin.,*2003, **102**, 386.
[49] D. Hreniak, W. Strek, P. Dereń, A. Bednarkiewicz, Łukowiak, *J. Alloys Compd*., 2006, **408 ,** 828.
[50] G. Blasse, B. Grambier, *Luminescent Materials, Springer-Verlag*, 1994, p.43.
[51] X. Xiao , B. J. Yan , *Mater Lett.,* 2007, **61** , 1649, 2007.
[52] D. V. Voort, A. Imhof, G. Blasse, *J. Solid State Chem.,* **96**, 311, 1992.
[53] Li-Li Shi, Yu Li Cheng, Su Qiang, *J. Fluorescence* **21**, 1461,2011.

Author Profile

Dr. Subhash Chand , is a senior research scholar in the Department of Chemistry , M.D.University Rohtak-124001, Haryana, India and working on nanomaterial synthesis since 2008. Dr. Subhash Chand had published five research paper in International Journal indexed with Thomson RSmter. He presented four paper in national conference. One research paper is presented and published in international conference held at MIMT, Kota, Rajasthan, India. He attended two national workshop and also participated two times in state level science exhibition.